energy&fuels

Article

pubs.acs.org/EF

Experimental Investigation of Spark-Ignited Combustion with High-Octane Biofuels and EGR. 1. Engine Load Range and Downsize Downspeed Opportunity

Derek A. Splitter* and James P. Szybist†

Fuels, Engines, and Emissions Research Center, Oak Ridge National Laboratory, NTRC Building, 2360 Cherahala Boulevard, Knoxville, Tennessee 37932, United States

ABSTRACT: The present study experimentally investigates spark-ignited combustion with 87 AKI E0 gasoline in its neat form and in midlevel alcohol−gasoline blends with 24% vol/vol isobutanol−gasoline (IB24) and 30% vol/vol ethanol−gasoline (E30). A single-cylinder research engine was used with an 11.85:1 compression ratio, hydraulically actuated valves, laboratory intake air, and was capable of external exhaust gas recirculation (EGR). Experiments were conducted with all fuels to full-load conditions with $\lambda = 1$, using both 0% and 15% external cooled EGR. Higher octane number biofuel blends exhibited increased stoichiometric torque capability at this compression ratio, where the unique properties of ethanol enabled a doubling of the stoichiometric torque capability with E30 as compared to 87 AKI, up to 20 bar IMEPg (indicated mean effective pressure gross) at $\lambda = 1$. EGR provided thermodynamic advantages and was a key enabler for increasing engine efficiency for all fuel types. However, with E30, EGR was less useful for knock mitigation than gasoline or IB24. Torque densities with E30 with 15% EGR at $\lambda = 1$ operation were similar or better than a modern EURO IV calibration turbo-diesel engine. The results of the present study suggest that it could be possible to implement a 40% downsize + downspeed configuration (1.2 L engine) into a representative midsize sedan. For example, for a midsize sedan at a 65 miles/h cruise, an estimated fuel consumption of 43.9 miles per gallon (MPG) (engine out 102 g-CO_2/km) could be achieved with similar reserve power to a 2.0 L engine with 87AKI (38.6 MPG, engine out 135 g-CO_2/km). Data suggest that, with midlevel alcohol−gasoline blends, engine and vehicle optimization can offset the reduced fuel energy content of alcohol−gasoline blends and likely reduce vehicle fuel consumption and tailpipe CO_2 emissions.

INTRODUCTION

The Energy Independence and Security Act[1] of 2007 requires that, by year 2022, 36 billion gallons per year of bioderived fuels need to be consumed in transportation. This uptake in bioderived fuels is a more than a 7-fold increase from the 4.7 billion gallons consumed per year when the law was enacted. The rules for complying with this mandate are specified by the U.S. Environmental Protection Agency (EPA) in the Renewable Fuel Standard II (RFS II).[2] When the total transportation energy consumption is analyzed, it is apparent that this legislation increases the usage of biofuels. In 2012 the United States consumed 27.97 quadrillion BTU of energy for transportation, and it is projected to consume 29.24 quadrillion BTU in 2022.[3] Assuming gasoline equivalent energy of 42.8 MJ/kg and density of 740 kg/m,[3] the RFS standard will require an increase in the percentage of transportation energy from biofuels to approximately 14% in 2022 from the approximate 2% in 2007. To date, the RFS II progress has seen more than a doubling of biofuel usage, with the annual recorded share of transportation energy from nonpetroleum sources totaling 4.3% in 2012. Although 2012 was the year with the largest biofuel energy share on record,[3] there is still an additional 3-fold increase in biofuel energy share required to comply with the RFS II mandate.

Concurrent with RFS II, legislation by the National Highway and Transportation Safety Administration passed in 2011 requires an effective 2-fold increase in corporate average fuel economy (CAFE) standards to achieve 54.5 U.S. miles per gallon by 2025,[4] an effective 2-fold increase compared with present CAFE standards. Ideally, The RFS II and CAFE mandates could be met simultaneously through proper exploration and implementation of high-efficiency biofuel engines.

In the United States, the stoichiometrically operated spark ignition (SI) engine has maintained over a 99% market share in the light-duty (LD) vehicle sector (passenger cars and pickup trucks) since 1985,[5] and over a 94% share since the EPA began record keeping in 1975. This LD sector engine dominance is due primarily to the facts that the SI engine has low production cost, low fuel cost, rugged operation, high power/torque density, low sooting tendency, and can employ known mature catalyst technologies to reduce regulated emissions (nitric oxide (NO_x), hydrocarbon (HC), and carbon monoxide (CO)). The market sector dominance with the SI engine in combination with legislated CAFE and RFS II standards suggests that increases to SI engine efficiency with biofuels might offer a very plausible path toward simultaneous CAFE and RFS II compliance.

Although the SI engine has many beneficial attributes, its efficiency is fundamentally hindered by the throttling of air, and its compression ratio is limited by combustion knock. These two factors result in lower thermal efficiency of SI engines relative to compression-ignited engines (i.e., diesel engines) or lean-burn SI engines. (Efficiency is defined as the efficiency of converting fuel chemical energy to mechanical output work.) Historically, engine

Received: August 7, 2013
Revised: December 21, 2013

   dx.doi.org/10.1021/ef401574p | *Energy Fuels* XXXX, XXX, XXX−XXX

improvements have focused primarily on increasing power safety and convenience, yielding increases in performance and vehicle weight, while complying with regular legislated fuel economy mandates, which have been near constant since 1985.[5] The progress in engine performance over the years can clearly be observed when viewed relative to a 1975 baseline (the first year of EPA records): in today's vehicles the industry average power-per-unit displacement has more than doubled, while vehicle 0 to 60 miles per hour acceleration time has halved.[5] This evolutionary increase in performance has resulted in a 50% reduction in the average modern light-duty engine displacement compared with a 1975 era engine. Although these trends show there has been significant progress in engine performance, to comply with future CAFE requirements, engine and vehicle efficiency must also be addressed and improved.

An evolutionary strategy for achieving CAFE compliance while retaining performance is downsizing and turbocharging with direct injection. These two technologies offer increased engine power/torque density, with equal or similar performance when downsizing and downspeeding of engines, a proven efficiency improving strategy.[6] However, the opportunity for downsizing and downspeeding becomes limited by combustion knock from the octane number and physical−chemical properties of current market-available fuels, thereby limiting thermodynamic efficiency.

Unlike distillate fuels, alcohol fuels exhibit some key properties that make them particularly attractive fuels for future engines. Most notably, alcohol fuels tend to have a high octane number and lower carbon intensity (defined as the number of moles of carbon per unit of energy (LHV)). These combinations of properties grant alcohol-based fuels a 2-fold reduction potential in tailpipe carbon dioxide (CO_2) through molecular advantage and the ability to tolerate higher engine compression ratios. Additionally, alcohol fuels exhibit two other properties that can be favorable for increasing engine efficiency:

First, alcohol fuels exhibit a high latent heat of vaporization (HoV), which, when used in conjunction with direct injection (DI) fueling, can increase the incoming charge density caused by a reduction in charge temperature. When exploited properly, the high HoV improves engine breathing, as highlighted by Stein et al.,[7] and mitigates combustion knock tendency. The effect of HoV has proved to be strong, even in a sparingly used dual-fuel arrangement, where the charge cooling of a small amount of direct-injected ethanol prevented knock and extended the torque capability,[8] with both benefits enabling higher efficiency engines.

Second, the amount of thermodynamic work that can be extracted from ethanol on a second law basis is higher than is suggested by its lower heating value (LHV) alone (i.e., exergy/LHV). This is attributed to a high yield of molar products for alcohols on both a stoichiometric and energy basis relative to petroleum distillates, increasing expansion pressure.[9,10] Ford and AVL have shown that ethanol enables efficiency improvements, with several notable works summarized in Stein et al.[11] Vehicle-specific effects were researched by Jung et al.[12] at light load conditions and also in an additional study by Jung et al.[13] with drive cycle and engine efficiency estimates. The latter study points out that a light-duty pickup truck engine with intermediate ethanol−gasoline blends could be optimized such that the thermal efficiency increase with ethanol−gasoline blends of 20% ethanol vol/vol are sufficiently high to at least offset the fuel mileage penalty of alcohol fuels (miles per gallon, [MPG]) and achieve even greater tailpipe CO_2 reductions.

These engine experiment and vehicle simulation results demonstrate that reductions in CO_2 emissions without a decrease in MPG could be possible with intermediate ethanol−gasoline blends. A major reason for this prediction is the ability of ethanol addition to reduce combustion knock and enable an increased compression ratio. Interestingly, work by Szybist and West[14] demonstrates that blending ethanol, even with very low-octane gasoline blendstocks, offers significant antiknock resistance and that a high-octane fuel can be produced through blending intermediate levels of ethanol with straight-run-gasoline. This is because of the highly nonlinear response of octane number blending with ethanol on a volumetric basis, as previously explained in detail by Anderson et al.[15,16] and more recently by Foong et al.[17] These cited studies show that intermediate-level ethanol blends might be promising for the next generation of SI engine fuels. The noted inherent benefits provide the potential to increase the power output and efficiency of the engine through fuel-based knock mitigation coupled with engine optimization. However, as pointed out in the 2013 SAE International High Octane Fuel Symposium,[18] multiple levels of cooperation from the fuel industry, legislation and regulatory bodies, distribution systems, and point of sale vendors are required if fuel octane number is to be increased.

The use of external cooled exhaust gas recirculation (EGR) could be a more direct approach to increasing SI engine efficiency. External EGR is a proven method to reduce the knocking tendency for a given fuel. External-cooled EGR has been employed for years in diesel engines, with recent interest gaining in SI engines. The constituents of EGR in SI engines differ from those in their diesel counterparts. Specifically, $\lambda = 1$ SI EGR is oxygen deficient, meaning that SI EGR offers the potential to increase charge mass without changing the oxygen content. The lack of oxygen in SI EGR is important when considering both catalyst and throttling requirements of SI engines (i.e., $\lambda = 1$). In addition to reducing throttling losses, the introduction of EGR into SI engines improves the thermodynamic properties of the working fluid (i.e., the ratio of specific heats [γ]), reducing in-cylinder temperatures and improving knock resistance.

Many of these thermodynamic advantages have been documented by others. For example, Alger et al.[19] showed that external-cooled EGR effectively decreased the knocking propensity of distillate fuel, which functionally increased the fuel octane number. However, EGR also slowed the flame kernel growth because of slowed reaction rates. Therefore, higher EGR levels in SI engines might require the incorporation of different higher turbulence combustion chamber flows to increase EGR tolerance, as shown by Wheeler at al.,[20] or through high-energy long spark systems, as shown by Alger et al.[21] These previous studies suggest that there are technical challenges that need to be addressed for implementation with current market fuels if EGR is to be used.

The relation between knock mitigation and cycle difference with external-cooled EGR raises several questions:

1. Can knock resistance of conventional distillate fuels be sufficiently improved to the levels of midlevel alcohol blends through the addition of EGR?
2. What, if any, role does EGR have on engine efficiency in midlevel alcohol blends?
3. What are the combustion-specific differences between intermediate alcohol−gasoline blends and neat gasoline?

dx.doi.org/10.1021/ef401574p | Energy Fuels XXXX, XXX, XXX−XXX

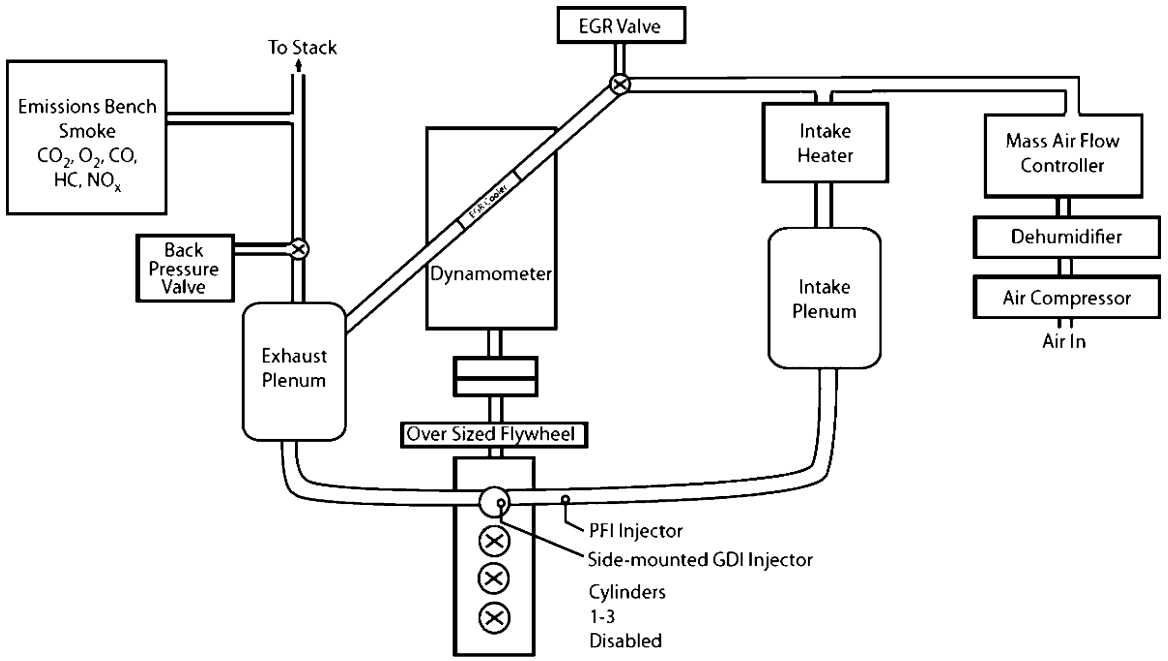

Figure 1. Schematic of the experimental configuration.

4. What, if any, potential performance and fuel economy incentives do midlevel alcohol−gasoline fuel blends offer, both with and without external-cooled EGR?
5. Can intermediate alcohol−gasoline fuel blends enable new powertrain possibilities?

This study is partitioned into two separate manuscripts. Both parts explore the use of midlevel ethanol and isobutanol gasoline blends compared with conventional gasoline, each with 0% and 15% external-cooled EGR. The current results (part 1) explore the engine efficiency, stoichiometric torque capability at high compression ratio, and downsizing + downspeeding potential of each fuel-EGR combination relative to one another; with E30+15% EGR also compared with high-efficiency conventional diesel engine data. In the companion study (part 2), a more detailed, combustion-specific approach is taken, in which combustion, thermal efficiency, and knock phenomena of each fuel−EGR combination are investigated.

EXPERIMENTAL DETAILS

This study explores SI engine operation at five engines speeds (1200, 1600, 2000, 2500, and 3000 r/min) and two different EGR rates (0% and 15%), each with three different fuels (87AKI E0 "regular" gasoline, 30% by volume ethanol−gasoline, and 24% by volume isobutanol−gasoline). A highly modified 2.0 L GM Ecotec SI engine with stock side-mounted direct fuel injector is used. Three cylinders of the production engine are disabled to allow single-cylinder operation with an installed custom-domed piston, which increases the compression ratio to 11.85:1 (stock 9.2:1). Notably, the increase in compression ratio changes many attributes of the combustion chamber geometry, therefore complicating a direct comparison of the higher compression ratio data to the stock compression ratio. Splitter and Szybist[22] discuss observed differences in combustion and emissions between the stock 9.2 and modified 11.85 compression ratio pistons, while the current study omits the direct comparison.

The SI engine is operated with a laboratory air-handling system. Pressurized and dried facility air that has less than 5% relative humidity is metered to the engine using a mass air-flow controller. The present study omits humidity effects, where added humidity may have an effect of reducing knock. The engine is equipped with separate electro-mechanical valves for backpressure and external EGR, enabling the capability for independent control of intake manifold pressure, exhaust manifold pressure, and EGR. Cooled EGR mixes with fresh air upstream of an air heater, followed by the intake plenum and then the intake manifold. EGR is measured using an EGR 5230 system from ECM, an instrument that uses pressure-compensated wide-band oxygen sensors in both the intake and exhaust to nonintrusively measure EGR. When EGR was used, a constant rate of 15 ± 1% was supplied. A schematic of the laboratory is provided in Figure 1.

The engine is equipped with a hydraulic valve actuation (HVA) system to enable fully variable valve actuation. To accommodate the small research module HVA system from Sturman Industries, the cylinder head has been machined, disabling the functionality of the production cam and fuel pump systems. Details of the HVA system have been published previously.[9,23,24] The engine geometry is listed in Table 1.

Table 1. Engine Geometry

bore × stroke	86 × 86 mm
connecting rod length	145.5 mm
compression ratio	11.85:1
fuel injection system	direct injection, side-mounted

Crank-angle (CA) resolved data are recorded at 1800 samples per revolution (0.2°CA resolution) for 300 consecutive cycles. Cylinder pressure is measured using a Kistler piezoelectric 6125B pressure transducer coupled to a Kistler 5010 charge amplifier. Additionally, the DI command signal and intake and exhaust valve lift from each of the four HVA valves is recorded on a crank-angle resolved basis. All indicated results presented in this study are for a 300 cycle average.

Engine emissions are measured using a standard emissions bench with instruments manufactured by California Analytical Instruments. NO_x emissions are measured using a chemiluminescence analyzer, CO and CO_2 are measured using infrared analyzers, oxygen (O_2) is measured using a paramagnetic analyzer, and HC is measured with a flame ionization detector. Smoke measurements are performed using an AVL 415s filter smoke number (FSN) instrument. To measure the fuel flow rate (and thus efficiency), the air-to-fuel ratio (AFR) is measured directly from a Coriolis-effect fuel flow meter and a laminar air flow element. The corresponding fuel flow is then cross referenced to

dx.doi.org/10.1021/ef401574p | Energy Fuels XXXX, XXX, XXX−XXX

independently calculate air-to-fuel ratios from the engine exhaust using both the emissions bench and automotive wide-band oxygen sensor approaches.

The conditions maintained for all fuels, engine speeds, loads, and EGR combinations are listed in Table 2.

Table 2. Constant Operating Conditions

exhaust valve open at 0.8 mm lift (°CA ATDC$_f$)	170
exhaust valve close at 0.8 mm lift (°CA ATDC$_f$)	350
max exhaust valve lift (mm)	9
intake valve open at 0.8 mm lift (°CA ATDC$_f$)	−355
intake valve close at 0.8 mm lift (°CA ATDC$_f$)	−170
max intake valve lift (mm)	9
start of DI command (°CA ATDC$_f$)	−280
intake manifold gas temperature (°C)	52
engine coolant (°C)	90
oil (°C)	90
exhaust λ	1
DI rail pressure (bar)	100

Five engine speeds of 1200, 1600, 2000, 2500, and 3000 r/min were tested, with gross load increments (IMEPg, indicating mean effective pressure gross) of 50 ± 5 kPa. The constraints and load range for E30 without EGR are seen in Figure 2, which illustrates the tested operational map up to the constraints for E30 with 0% EGR. The identical procedure and setup is conducted for each fuel type and both EGR rates.

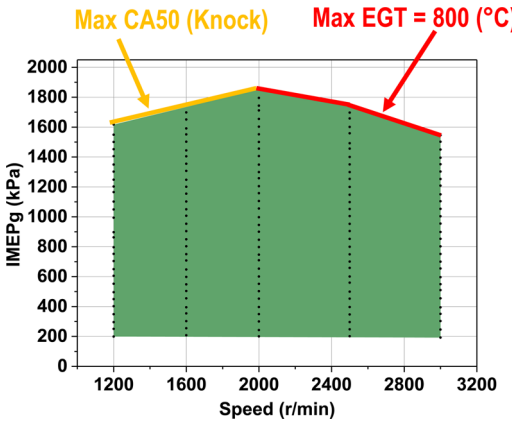

Figure 2. Representative engine load-speed range tested with knock and EGT constraints indicated.

All fuels and EGR rates are tested at maximum brake torque (MBT) timing until combustion knock is encountered. Once knock limited, combustion is phased through spark timing to maintain a constant level of knock through visual inspection of the indicated pressure trace and by maintaining constant AVL combustion noise. The tested load range is from 2 bar IMEPg to full load, which is defined as the maximum load without enrichment (λ = 1) with limits on CA50 (crank angle at 50% mass fraction burned) combustion phasing of 25°CA ATDC$_f$, peak cylinder pressure of 10 000 kPa, and exhaust gas temperature (EGT) of 800 °C. (Note: CA50 combustion phasing later than 25°CA ATDC$_f$ is not ideal for high efficiency, which is the focus of the present study. Additionally, an 800 °C EGT limit is imposed because, unlike the production engine, the Sturman valvetrain does not use sodium-filled values which can withstand higher exhaust gas temperatures. The maximum cylinder pressure limit is set because the stock engine is rated to 10 000 kPa, although this constraint is not reached by any of the present fuel or experimental condition combinations.) Figure 2 displays the constraint limits reached with 0% EGR E30 operation.

The only exception to the constraints is at the lightest loads with EGR (IMEPg ≤ 250 kPa), where combustion is unstable at MBT CA50 phasing, where later than MBT CA50 were found to improve stability. The constraint used to bound the amount of CA50 retarded for acceptable operation at these lightest loads is CA50 ≤ 15 °CA ATDC$_f$. Using these limits, operation with each fuel is compared.

The production spark plug heat range and gap are used for all tests. However, the spark energy is generated with an aftermarket MSD DIS6-2 Plus multistrike ignition system to increase the combustion stability at high EGR levels. The MSD system is capable of up to three consecutive spark discharges per cycle, but the number of discharges is speed dependent, with only one or two discharges at higher engine speeds. The spark coil signal from the MSD system, heat release rate (HRR), and cylinder pressure are indicated in Figure 3, along with the unique valve

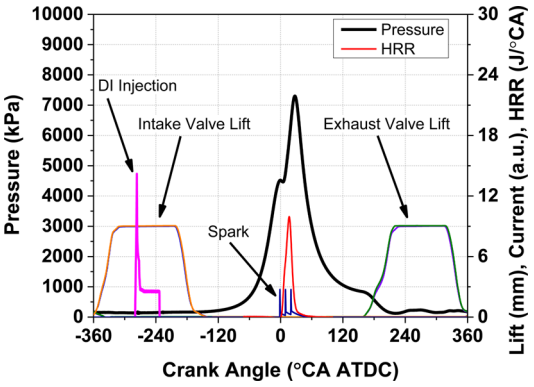

Figure 3. Representative high-load fired case showing indicated cylinder pressure and apparent HRR with corresponding valve, spark, and injection event schedule.

events provided by the Sturman HVA system. The near square valve lift profile generated by the Sturman HVA system differs from conventional valve lift and duration dynamics, resulting in increased flow area with different engine breathing and charge motion characteristics. The specific differences between the HVA valvetrain and a cam-based valvetrain are discussed in a previous publication.[24]

When operating with higher than atmospheric pressures, a constant overall turbocharger efficiency of 25% with no intake or exhaust pressure restrictions is assumed (i.e., no muffler pipe, catalysis, or air cleaner pressure losses assumed). This assumption is considered valid and conservative because the production turbocharger for this SI engine is capable of over 55% combined overall efficiency. The combined turbocharger efficiency is calculated based on the air standard model as explained by Heywood[25] (eq 1), using intake and exhaust surge tank pressures and temperatures measured in the ports and assuming 100% turbine shaft mechanical efficiency. When operating with external EGR, the electromechanical valves for backpressure and EGR were modulated as needed to maintain 15% EGR and 25% combined turbocharger efficiency.

Overall turbocharger efficiency calculation

$$\eta_{\text{combined}} = \frac{\left(\frac{\gamma_{\text{comp}}}{\gamma_{\text{comp}}-1}\right)\left(\frac{T_{\text{comp,in}}}{T_{\text{turb,in}}}\right)}{\left(\frac{\gamma_{\text{turb}}}{\gamma_{\text{turb}}-1}\right)} \frac{\left[\left(\frac{P_{\text{comp,in}}}{P_{\text{comp,out}}}\right)^{[(\gamma_{\text{comp}}-1)/\gamma_{\text{comp}}]}-1\right]}{\left(1+\frac{1}{\text{AFR}}\right)\left[\left(\frac{P_{\text{turb,out}}}{P_{\text{turb,in}}}\right)^{[(\gamma_{\text{turb}}-1)/\gamma_{\text{turb}}]}\right]} \quad (1)$$

Fuels and Fuel Properties. Three fuels are tested: two fuels are alcohol−gasoline blends, and the third is an unblended gasoline. The

dx.doi.org/10.1021/ef401574p | Energy Fuels XXXX, XXX, XXX−XXX

two alcohol blended fuels were splash blended on site with either 24% neat isobutanol or 30% neat-ethanol, with alcohol and gasoline volume fractions being measured in unblended fractions and then combined. All fuels were based on commercially obtained 87 AKI E0 "regular" pump fuel sourced directly from a distribution terminal. It should be noted that splash blending these alcohols with finished market E0 gasoline is not likely at an industrial scale if the tested blend ratios were to be market sold. More likely, a blendstock for oxygenate blends (BOB) fuel would be used, which tend to have lower octane numbers. Although using a BOB would decrease the research octane number (RON) of a blended fuel below those tested in the present study, others studies,[7,14] have shown that the RON difference of a blended fuel based on a BOB vs a finished E0 is much smaller than the difference in RON between the unblended BOB and finished E0 fuels.

The blending ratios used are based on the following:

- 24% isobutanol was selected, as it has near identical oxygen content as E15, which the EPA has approved for use in 2001 and newer light duty vehicles.[26,27]
- The 30% ethanol blend was selected because, as the EPA recently stated,[28] there is no foreseeable issue with higher ethanol−gasoline blends; citing blends as high as E30 would likely be permissible.

These alcohol−gasoline fuel blends are of interest, as the neat alcohols used exhibit nearly identical motor octane number (MON) values and similar RON values.[29] However, the energy density of isobutanol is higher than that of ethanol on both a volume and mass basis, thus making its energy density closer to that of a gasoline. Additionally, the lower water solubility of isobutanol as compared to ethanol offers advantages in certain markets such as marine environments where humidity and water contact are more prone. Interestingly, research by Stein et al.[11] has demonstrated that the Reid vapor pressures of intermediate ethanol blends are typically lower than those of E10 blends for the same blendstock, making such fuels attractive to regulatory bodies, as has been indicated in the recent EPA Tier III notification of proposed rulemaking.[28]

In the present study, the alcohols are from nondenatured reagent grade purity and obtained directly from suppliers. Sigma-Aldrich supplied the isobutanol at a purity of >99%, and Decon Laboratories supplied the nondenatured ethanol. The three fuels were sent for independent analysis at an ASTM international-certified laboratory. The key chemical properties from the analysis are presented in Table 3, which shows that the fuels have significantly different chemical and physical properties.

This paper discusses an opportunity to achieve higher engine efficiency by taking advantage of renewable fuel properties. If a lower carbon renewable fuel can be used with higher engine efficiency, this could enable simultaneous compliance with RFS II and CAFE, as well as foster a technological codependence between renewable fuels and highly efficient engines that would set the sustainable transportation trajectory to extend beyond the requirements set by RFS II and CAFE legislation.

RESULTS

This section is divided into four subsections. The first provides an overview of the fuel-specific differences on the operable speed-load range of the engine without EGR, while the second provides this information with EGR. The third provides the results of converting the data to brake thermal efficiency in a multicylinder engine, along with the methodology for the calculation. The final subsection discusses downsizing and downspeeding implications.

Speed-Load Range Overview. All fuels are operated to the maximum load condition defined by the aforementioned combustion knock and EGT constraints. The tested load range of the three fuels with 0% (solid) and 15% (hashed) EGR is presented in Figure 4. 15% EGR was used because it is empirically found to have robust and acceptable combustion characteristics over the load-speed range of interest.

Table 3. Fuel Properties

	87 AKI	IB24	E30
oxygenates ASTM D5599 (% v)	<0.1 any	23.64 isobutanol	30.65 ethanol
HoV (kJ/kg)[a]	352[29,30]	443[29,29,31]	529[29,29,31]
HoV with gasoline energy equiv[b] (kJ/kg)	352[29,30]	470[29−31]	599[29−31]
Reid vapor pressure, ASTM D5191 (psi)	13.13	12.29	13.28
10% distillation point, ASTM D86 (°C)	97	115	111
30% distillation point, ASTM D86 (°C)	144	175	150
50% distillation point, ASTM D86 (°C)	205	208	165
70% distillation point, ASTM D86 (°C)	253	222	170
90% distillation point, ASTM D86 (°C)	316	307	299
RON, ASTM D2699	90.2	96.6	100.3
MON, ASTM D2700	83.9	86.8	88.8
sensitivity	6.3	9.8	11.5
LHV, ASTM D240 (MJ/kg)	43.454	40.846	38.105
λ = 1 AFR	14.70	14.13	12.85
C, ASTM D5391 (wt %)	86.49	80.63	74.4
H, ASTM D5391 (wt %)	14.06	13.89	13.73
O, ASTM D5599 (wt %)	<0.1	3.71	11.34
specific gravity, ASTMD 4052	0.729	0.7423	0.745
volumetric energy density (MJ/gal)	119.5	114.5	107.1

[a]Calculated through a linear combination of neat alcohol and neat gasoline HoV. [b]Calculated on a gasoline equivalent energy basis (i.e., required for matched load).

The results displayed in Figure 4 show that the higher octane fuels attain improved stoichiometric torque capability at high compression ratio, particularly with E30, regardless of the presence of 15% EGR. The specific reasons for this are investigated in greater detail in the companion paper (part 2). The present analysis addresses application- and performance-level differences of each fuel in an SI engine.

To better understand the performance of the three fuels, the gross thermal efficiency (GTE) contours with 0% EGR are plotted as functions of speed and load in Figure 5. Note the knock limit in the contours, denoted by a thick dashed black line in the figure (loads above the knock limit use combustion phasing between MBT and the 25°CA ATDC$_f$ limit).

The results illustrate that GTE increases with engine speed and that the maximum GTE of a given speed resides at the knock limit for all fuels. Additionally, as knock resistance increases, the islands of higher GTE increase by stretching toward lower engine speeds and higher IMEP. This demonstrates that there is merit for increasing the fuel octane, especially with intermediate ethanol−gasoline blends, at least from a gross efficiency and stoichiometric torque capability at high compression ratio basis. Furthermore, the load range under knock-limited operation with E30 is significantly larger than 87 AKI gasoline or IB24. The specific reasons for this increased knock limited stoichiometric torque capability at high compression ratio are addressed in detail in the companion study, part 2, where fuel octane effects are addressed.

Speed-Load Range Overview: With 15% EGR. It is well established that the addition of cooled external EGR increases efficiency.[19,21,34] The results presented in this study support previous findings on the effect of EGR. A GTE analysis is useful

dx.doi.org/10.1021/ef401574p | Energy Fuels XXXX, XXX, XXX−XXX

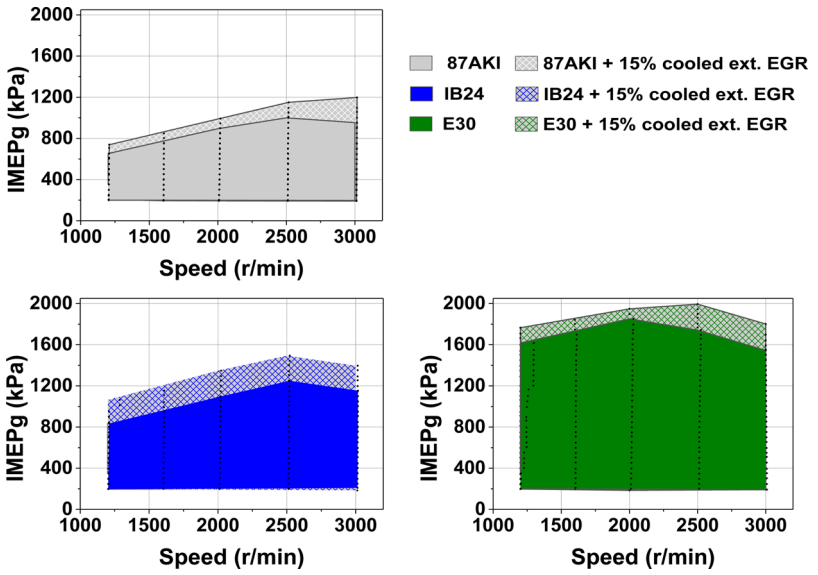

Figure 4. Gross load range of the tested fuels with 0% EGR operated to the constraints shown in Figure 2.

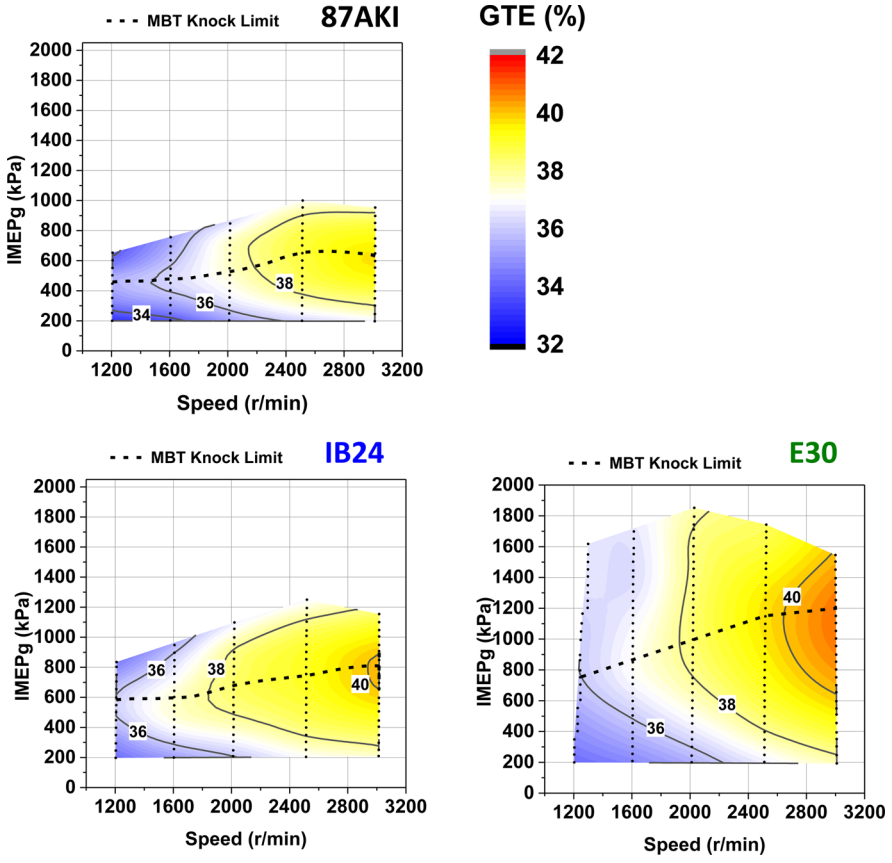

Figure 5. Contours of gross thermal efficiency and load range of the tested fuels with 0% EGR. The dashed heavy line in each graph indicates the MBT knock limit. The small dots indicate measured data points.

for determining how EGR impacts thermal losses and combustion processes. For comparison, the GTE of each fuel with 0% EGR was subtracted from operation with 15% EGR. The resulting difference in GTE with 15% EGR is plotted in Figure 6 (ΔGTE). The additional load enabled with 15% EGR is also shown in the figure, represented by the gray shading.

The results illustrate that the advantages of EGR are approximately the same for each fuel studied. Gains in GTE at the mid and higher loads are observed to be on the order of 2−3 points absolute. For IB24 and 87AKI, the highest gains in efficiency occur near the peak torque, where, in addition to its other thermodynamic advantages, combustion phasing is more knock-limited without EGR and the presence of EGR permits a more advanced combustion phasing. However, for E30, there is a diminished benefit of EGR at high loads. This is believed to be a fuel-specific effect, where the companion paper (part 2) found

dx.doi.org/10.1021/ef401574p | *Energy Fuels* XXXX, XXX, XXX−XXX

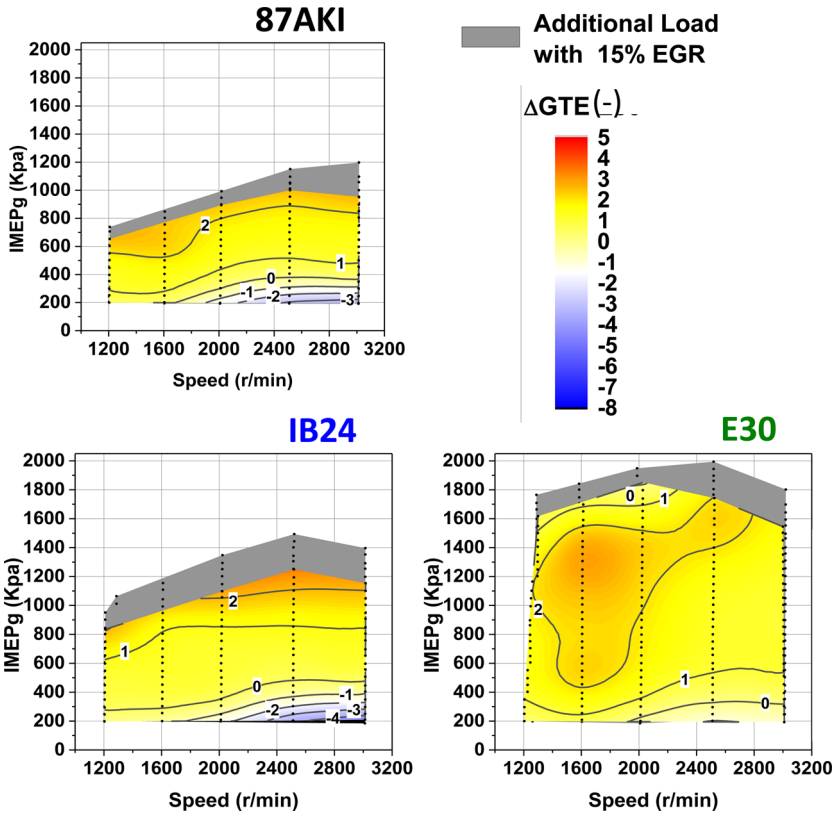

Figure 6. Contours of absolute percentage point increase in gross thermal efficiency with 15% EGR addition. The gray shaded region illustrates the increase in load range with 15% EGR vs 0% EGR.

that EGR was less effective at knock mitigation in E30 than the other tested fuels.

Unlike the fuel-specific effects at high load, at light loads (i.e., 2 bar IMEPg) EGR was found to be more detrimental to efficiency for each fuel, especially at higher engine speeds. This detrimental effect can possibly be attributed to the poor flame kernel growth present with dilute combustion, which exasperates at higher engine speeds. More detail on these attributes is provided in the companion paper, part 2.[32]

Calculating Brake Thermal Efficiency. The previous analysis illustrates that, from a gross basis, EGR offers significant advantages. However, it does not include the pumping or friction work needed to estimate brake thermal efficiency. As stated, all tests are conducted on a single-cylinder engine, and while these engines are best at offering a highly controlled research environment as cylinder-to-cylinder interactions are removed, the frictional losses from single-cylinder engines are often much larger than those from multicylinder engines. For example, the test engine in the present study has three deactivated cylinders. These cylinders still rotate, generating tribology losses, but they have zero compression. Therefore, direct dynamometer power measurements are biased to be lower on the test engine than in production multicylinder engines. Thus, it is common to correlate indicated (cylinder pressure-derived) power and performance to brake performance (shaft output) with a friction correlation. The friction mean effective pressure (FMEP) is calculated from the indicated data using the same correlation in the Gamma Technologies Power (GT Power) commercial code.[33] The correlation is shown in eq 2, where the terms C_1−C_4 are constants with the values given in Table 4, PCP represents the peak cylinder pressure, and $\overline{P}_s$ represents the mean piston speed. Note that the present study uses the default GT Power values for constants C_1−C_4. Using the default FMEP constant values, good agreement between the correlated BMEP and BTE of the present single-cylinder engine is made to chassis dyno testing of the production vehicle and engine (Figure 14), justifying the use of the default values.

Table 4. FMEP Constants Used in This Study

C_1 (bar)	0.04
C_2 (bar)	0.005
C_3 (bar)	0.09
C_4 (bar)	0.0009

$$\text{FMEP} = C_1 + (C_2 * PCP) + (C_3 * \overline{P}_s) + (C_4 * \overline{P}_s^2) \quad (2)$$

The resulting FMEP for E30 operation with 0% EGR is plotted in Figure 7. Note that FMEP increases with engine speed and that, as load increases, the FMEP lines turn from diagonal to vertical. The speed dependency occurs from increases to mean piston speed, while the vertical trend at mid-to-high loads occurs from reduced or constant PCP from knock limited retarded combustion phasing.

When approximating brake mean effective pressure (BMEP), pumping work considerations are required. Similar to FMEP, pumping can be normalized by engine displacement and be expressed as a pumping mean effective pressure (PMEP). PMEP can be especially high when the intake charge is throttled in SI engines. Since throttling only affects the gas exchange process, gross thermal efficiency is unaffected. However, when considering the entire 720° crank angle duration of all four strokes, the gross efficiency is reduced by the PMEP and the net thermal efficiency (NTE) is calculated.

dx.doi.org/10.1021/ef401574p | *Energy Fuels* XXXX, XXX, XXX−XXX

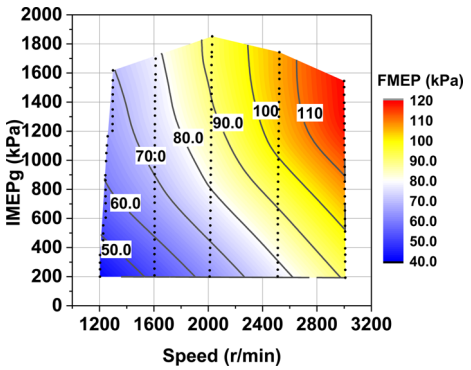

Figure 7. Contours of FMEP determined with eq 1 as functions of load-speed range for E30 with 0% EGR.

In SI engines with $\lambda = 1$ requirements, the piston force imbalance from throttling can be mitigated through the introduction of inert diluent (i.e., EGR), which raises the in-cylinder pressure without changing the intake oxygen concentration. The reduction in PMEP with EGR translates to an increase in NTE but has no effect on GTE. This presents a 2-fold effect that EGR can have on SI engine efficiency. First, it can increase GTE through phasing and thermal effects (see Figure 6), and it can increase NTE through reduced PMEP. The PMEP and FMEP are plotted as functions of load in Figure 8 for E30 operation with and without 15% EGR. Note that both PMEP and FMEP are energy sinks, where higher magnitudes correspond to increased losses.

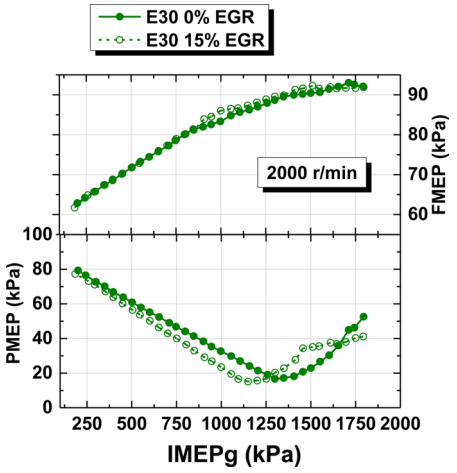

Figure 8. PMEP and FMEP of E30 with and without EGR at 2000 r/min engine speed.

The results illustrate how intrinsic fluid dynamic and mechanical losses are introduced when different portions of the engine efficiency metrics are used. Of interest is the reversal of the PMEP trend at higher loads. This is because of the 25% overall turbocharger efficiency assumption, where larger increases in backpressure are required to drive EGR, which increases PMEP and thus efficiency loss.

Using the measured PMEP and correlated FMEP, net and brake MEP and respective efficiencies can be estimated. The brake numbers represent the available work from the crankshaft and are noted as BMEP and brake thermal efficiency (BTE), respectively. The results are plotted in Figure 9, displaying the breakdown in BTE, NTE, and GTE as functions of IMEPg.

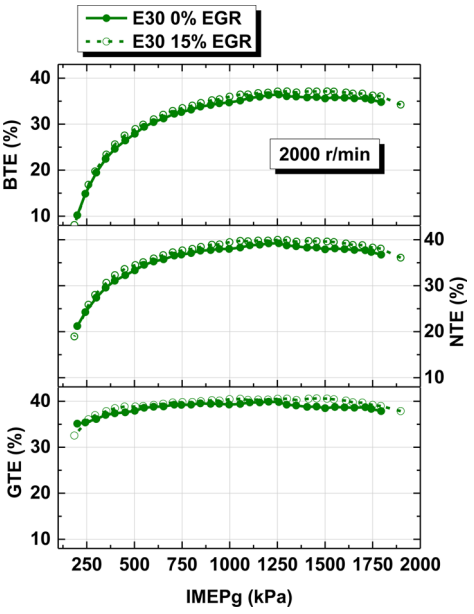

Figure 9. Efficiencies of E30 with and without EGR at 2000 r/min engine speed for different definitions of engine thermal efficiency.

The results illustrate the sources and losses of net brake and gross efficiencies with EGR. Specifically, with 15% EGR the GTE is slightly increased (except for the lowest loads where EGR operation is unstable and phased later). The increase in GTE is primarily because of the thermodynamic advantages of EGR in terms of γ and reduced in-cylinder temperatures, as pointed out by simulations by Caton[34] and in experiments by Alger et al.[21] and Szybist et al.[10] These thermodynamic and working fluid advantages offer fundamentally derived increases to gross and net engine fuel efficiencies.

The difference in NTE is derived only from the pumping differences, which are displayed as the reduction in PMEP with EGR in Figure 8. PMEP is negatively affected with EGR (turbocharger assumptions resulted in increased backpressure) only at the highest loads. For all lower loads in the sweep, the reduction in PMEP with 15% EGR (Figure 8) compounds on the GTE advantage with EGR, further increasing NTE. Additionally, Figure 8 shows that the FMEP penalty with 15% EGR is only marginally higher. The FMEP increase occurs because the additional charge mass with EGR can increase the peak cylinder pressure. As seen, this effect is relatively small, with BTE trends matching NTE trends, and the increased charge mass effects on PCP are likely mitigated from EGR, also reducing peak burned gas temperatures and, thus, pressure.

All of the gross, net, and brake efficiency results demonstrate that EGR has several levels of interaction on engine efficiency. This codependent relationship becomes more evident when the calculated BTE of operation with 87AKI+15% EGR is compared with 0% EGR operation with either of the two alcohol blends. These comparisons are presented in Figure 10, where the absolute percentage of BTE increase is defined as the BTE of 87AKI+15% EGR minus the BTE of the respective alcohol blend with 0% EGR.

The results show that the distillate fuel with 15% EGR can achieve a similar stoichiometric torque capability at high compression ratio to the IB24 blend with 0% EGR and between a 1 and 2% increase in absolute BTE relative to either alcohol blend with 0% EGR. However, as compared with E30, 87AKI +15% EGR exhibits an approximate 40−50% reduction in

dx.doi.org/10.1021/ef401574p | *Energy Fuels* XXXX, XXX, XXX−XXX

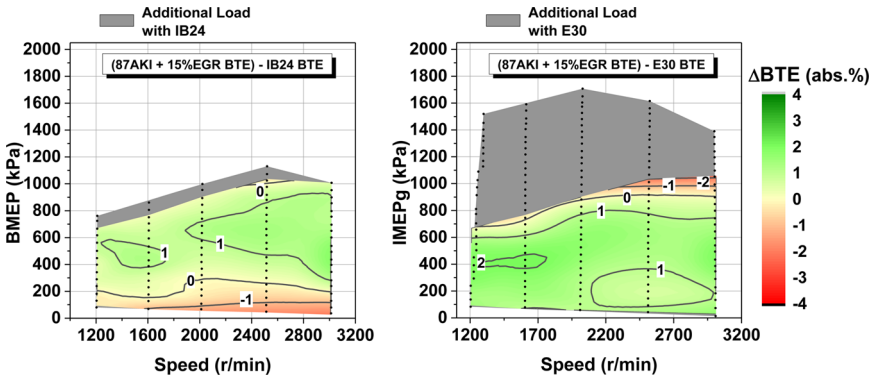

Figure 10. Contours of increase in BTE of 87 AKI gasoline + 15% EGR relative to 0% EGR with IB24 (left) and E30 (right). The gray shaded area is the increase in load range that was achieved with IB24 or E30, respectively.

maximum load, and at higher 87AKI+15% EGR loads, the BTE advantage could actually be negated because of knock-limited operation. The results of Figures 8–10 show that 15% EGR with 87AKI can approximately match the load-speed range (i.e., antiknock properties) of IB24 but is insufficient to match the load-speed properties of E30. However, 15% is observed to increase BTE from PMEP reductions and GTE increases. However, unlike PMEP effects, the differences in GTE were found to be fuel dependent, which merits more investigation. A detailed investigation is presented in the companion paper (part 2). The present study investigates vehicle application level analysis of the tested fuels.

Downsizing and Downspeeding Implications. As stated in the Introduction, the evolutionary progression of the internal combustion engine has led to smaller displacement and higher power/torque density engines. Higher octane biofuels might be enabling technologies to meet mandated CAFE standards and RFS II quota. In this section the potential benefits of midlevel alcohol–gasoline biofuels are assessed using a single representative vehicle road load and highway cruise analysis.

As shown in Figures 9 and 10, EGR use should be considered as a method to maximize engine BTE. A comparison with 15% EGR between E30 and 87 AKI is presented in Figure 11, where two gray lines are overlaid that depict constant 16 kW power for 2.0 and 1.2 L engines, respectively. The test engine is a 4-cylinder 2.0 L combined displacement platform, in which the 2.0 L constant power line is generated by multiplying the measured single-cylinder values by 4. The 1.2 L power line was determined

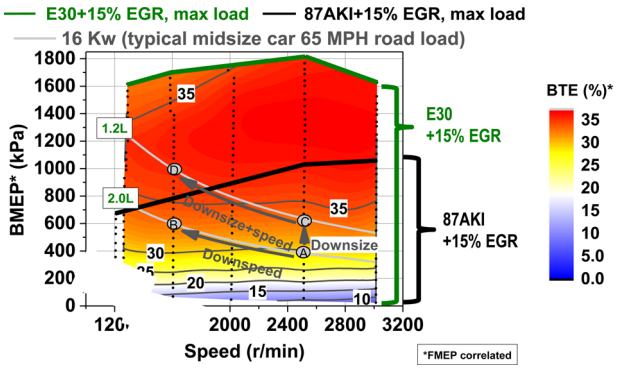

Figure 11. Contours of brake thermal efficiency and load range of 87 AKI E0 and E30, each with 15% EGR. Note that points A, B, C, and D are presented, along with lines of constant 16 kW power for 2.0 and 1.2 L engines.

using the assumption that equal FMEP and thermal losses exist in a 1.2 L platform, enabling a proportional downscaling of the power output.

Also presented in Figure 11 are four points: A, B, C, and D. Point A represents a midsize sedan with a 2.0 L engine and a final drive ratio such as at 65 mph equated to 2500 r/min engine speed at 16 kW. The road load is determined from EPA chassis dynamometer data,[35] by averaging two of the bestselling midsize US sedans in 2012. Point B represents the same cruise condition but with a downspeeded engine created by changing the final drive ratio/transmission. Point C represents a downsized engine of 1.2 L with the same final drive/transmission ratio as point A. Lastly, point D represents the 1.2 L engine in conjunction with a downspeed final drive ratio/transmission equal to that of Point B.

Although this simple approach is far from a full drive cycle estimate, the results clearly demonstrate that if downsizing and downspeeding are to be pursued—the current trend in the automotive sector—then high-octane biofuels can enable significant improvements. Clearly, with an 11.85:1 compression ratio (r_c), 87AKI+15% EGR gasoline is not capable of condition D and has marginal power reserve for load changes such as grade or aero load increases at conditions B and C. To enable the same drivability of condition A at conditions B, C, or D, the compression ratio of the engine would need to be reduced to the stock 9.2:1 r_c. Although this would enable operation or improve drivability, the BTE would be reduced, as the thermodynamic advantage of the engine cycle would also be reduced, as demonstrated by Szybist et al.[10,23] For a direct comparison, operation of 87AKI with the stock 9.2:1 r_c piston is presented by Splitter and Szybist,[22] which demonstrates that, at a 2000 r/min 500 kPa IMEPg load, the stock 9.2:1 r_c piston has a 3.8 point lower maximum Otto cycle efficiency [$\eta_{Otto} = 1 - (1/r_c^{(\gamma-1)})$] than the 11.85:1 r_c piston, a 11.1% relative reduction in BTE. Therefore, if increases to engine BTE are of pinnacle importance in the coming years, improvements to the fuel infrastructure might be required to enable high efficiencies and power densities.

Compared with 87AKI+15% EGR, E30+15% EGR can better use the downsized + downspeed configuration of condition D, while maintaining similar shift point requirements to 87AKI +15% EGR at the "standard" engine/transmission configuration of condition A. In other words, a near equal amount of reserve power ($\lambda = 1$) is available for dynamic load changes with E30 at condition D as there is with 87AKI+15% EGR at condition A. This enables a significant amount of flexibility in the optimization for downsized + downspeed arrangements.

dx.doi.org/10.1021/ef401574p | *Energy Fuels* XXXX, XXX, XXX–XXX

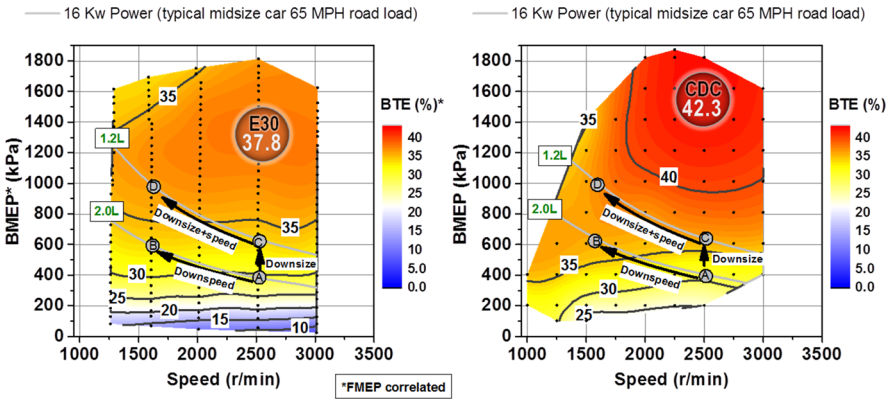

Figure 12. Contours of BTE and load range of E30+15% EGR (left) and EURO IV calibration CDC (right). Note, that points A, B, C, and D are presented, along with lines of constant for 16 kW power for a 2.0 and 1.2 L engine.

To demonstrate the stoichiometric torque capability at high compression ratio and BTE offered by E30, operation of E30+15% EGR was compared with conventional diesel combustion (CDC) in Figure 11. It is well-known that CDC is highly efficient and has high torque capability at low engine speeds. To compare the results, CDC operation by Curran et al.[36] on a production multicylinder engine with a Euro IV calibration with measured BMEP and BTE was selected (i.e., not correlated from indicated measurements using eq 1). The CDC operation was fueled with certification #2 ultralow sulfur diesel (it should be noted that the top rated speed for the engine used in those experiments was 4500 r/min, disregarded in the present analysis). Note, this comparison negates differences in losses that may occur when extrapolating single-cylinder results to a multicylinder engine configuration, as well as engine design and calibration differences that exist between compression and spark ignition engines. Nonetheless, comparing BTE maps between E30 and CDC provides a very preliminary illustrative and qualitative analysis between similar displacement high torque density engines that gives insight into powertrain opportunities.

The results displayed in Figure 12 show that in terms of low-to-mid engine speeds the load range E30+15% EGR at $\lambda = 1$ has, at least, an equal stoichiometric torque capability at high compression ratio to that of a turbo-diesel engine. Additionally, unlike CDC, SI is not mixing limited. Therefore, the low-speed, high-load operation of SI E30+15% EGR (1200 r/min) is not smoke limited, enabling even higher power/torque densities than those of CDC. Likewise, the high-speed range (i.e., power) is extended because SI does not become mixing rate limited (but enrichment might be required for catalyst thermal protection). Regardless of torque and power densities, the BTE at a given condition with CDC is higher because of fundamentally different engine and combustion processes. A direct comparison of the BTE difference is provided in Figure 13, where the BTE of E30+15% EGR is subtracted from the BTE of CDC.

Figure 13 illustrates that CDC has a 2−4% BTE advantage when throttling losses are minimal for E30+15% EGR (BMEP of $\geq$ ~400 kPa). A much greater advantage exists at BMEP below ~400 kPa, as throttling effects become more dominant in SI operation at this level. However, it is interesting to note that, at low speeds and high loads, E30+15% EGR is not smoke limited at lower loads (FSN $\leq$ 0.005) and thus can achieve higher BMEP at engine speeds below ~2000 r/min (see solid green region Figure 13). The low sooting tendency of SI engines offers a key advantage for downsized + downspeed configurations, as long as

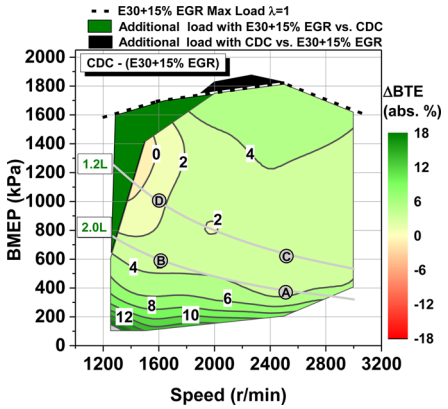

Figure 13. Absolute BTE advantage of CDC vs E30+15% EGR.

low-speed preignition (LSPI) can be avoided. Research by Amann et al.[37] has shown that EGR either reduces or possibly eliminates LSPI tendency. The present study did not observe any instances of LSPI with any tested fuel−EGR combination.

Additionally, note that the trends in Figure 13 are dependent on the assumption of 25% maximum overall turbocharger efficiency and FMEP of the E30+15% EGR map. The assumptions used are reasonable (FMEP in Figure 7 and 25% overall turbocharger efficiency) because the peak BTE of the present study is nearly identical to that obtained by Jung et al.,[13] which measured brake-based numbers from a multicylinder engine with a near identical compression ratio (11.9 vs 11.85) and fuel (E30).

The results in Figures 10−13 show that the brake efficiency and stoichiometric torque capability at high compression ratio of E30 are greatly improved over 87 AKI, achieving a similar torque capability to CDC. Although these comparisons demonstrate that downsized + downspeed engines are more enabled with E30+15% EGR, the findings displayed in Figures 10−13 do not show the possible impact on fuel consumption and engine out CO_2 emissions.

To estimate the possible impact on fuel economy and engine out CO_2 emissions, the steady-state MPG fuel consumption estimate and engine out CO_2 emissions are calculated from the FMEP correlated brake engine performance for 87 AKI and E30, both with and without EGR. Additionally, direct engine dyno measurements are used for BMEP and BTE of the production EURO IV engine,[36] and a low NO_x and noise CDC map (i.e., lower efficiency) are also compared. To reference the engine

dx.doi.org/10.1021/ef401574p | *Energy Fuels* XXXX, XXX, XXX−XXX

dyno-based MPG estimates to actual vehicle MPG, chassis dyno-measured MPG data were added (pink dashed line). The vehicle chassis dyno data are from Thomas et al.,[3839] at steady-state 65 MPH (2230 r/min in top gear) cruise using the production vehicle engine version of the present highly modified 2.0 L HVA single-cylinder SI engine and SI engine with E0 certification gasoline. The results of the comparison are presented in Figure 14.

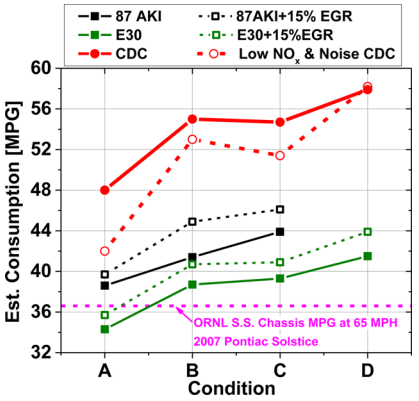

Figure 14. Estimated MPG of each fuel and combusiton strategy in a midize sedan at a 65 MPH steady cruise condition, referenced to chassis dyno data of the production GM Ecotec SI engine and vehicle.

Although the data in Figure 14 present the differences in the MPG calculations, there is surprisingly good agreement at condition A between the correlated engine dyno to vehicle MPG (pink dashed line) and the directly measured production vehicle chassis dyno MPG data (solid black line). Figure 14 shows that, at condition A, there is an approximate 3 MPG reduction in fuel economy with the production vehicle chassis dyno compared to the estimated single-cylinder to multicylinder to vehicle MPG with 11.85 r_c. This result is very similar to the predicted BTE difference associated with compression ratio effects in Splitter and Szybist;[22] thus, the results of Figure 14 demonstrate that the broad estimation scheme used to correlate single-cylinder dyno indicating engine data to vehicle MPG is at least reasonable. Note that as powertrain assumptions different from the production vehicle are assumed (conditions B–D), the trends begin to deviate, as expected.

Interestingly, the 87AKI at condition B has a lower relative MPG than other fuels at that condition. This is because it is at a CA50 of 25° CA ATDC$_f$ (at the phasing constraint of this study), and the efficiency reduces as phasing is retarded. Note that the steady-state MPG in Figure 14 is an unadjusted estimate, which is not representative of the adjusted MPG commonly reported in EPA fuel economy (i.e., window sticker fuel economy). Unadjusted EPA fuel economy is determined through weighting measurements with several different prescribed transient drive cycles on a laboratory chassis dynamometer.[35] To determine the adjusted MPG from the drive cycle average, a weighting factor is applied to estimate real-world predicted fuel economy (to account for weather, grade, etc).[40] This type of comparison is beyond the scope of the present study; however, it is noteworthy that CAFE is legislated on unadjusted MPG,[4] which was demonstrated to closely agree with steady-state dyno chassis testing,[39] adding merit to the present comparison.

To better demonstrate the efficiency trends, the unadjusted steady-state MPG is normalized to a gasoline equivalent basis (G eq. MPG) in Figure 15. Doing so removes volumetric fuel energy density from the determination of MPG, resulting in a comparison of brake engine efficiency.

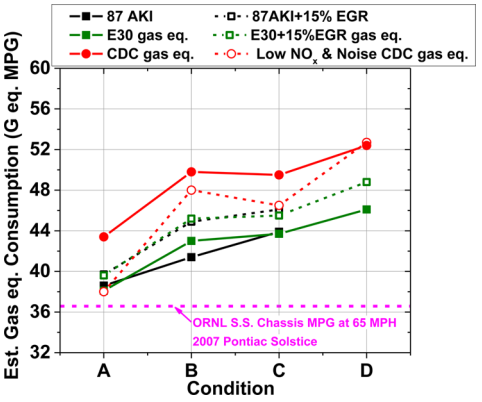

Figure 15. Estimated gasoline equlivalant MPG of each fuel and combustion strategy in a midsize sedan at a 65 MPH steady cruise condition, referenced to chassis dyno data of the production GM Ecotec SI engine and vehicle.

The results demonstrate that as each fuel type approaches a similar gasoline equivalent MPG (i.e., brake engine efficiency), vehicle efficiency becomes more dependent on EGR or the combustion process (i.e., CDC vs SI) rather than fuel type. Interestingly 0% EGR operation with E30 and 87AKI does deviate at condition B, where 87AKI is heavily knock limited (Figure 11). This demonstrates that although the efficiencies might be similar, the production viability might not be.

The results of this study further suggest that the carbon intensity of the different fuels affects the engine out CO_2 emissions similar to the way volumetric energy density differences affect MPG. In the present study, only engine out (uncatalyzed) emissions are measured. Regardless, nearly all of a vehicle's CO_2 emissions are produced by the engine before exhaust gas catalysis. The CO_2 emissions of conditions A, B, C, and D are compared in Figure 16 with 87AKI and E30, both with 0 and 15% EGR, and plotted with CDC data from Curran et al.[36]

The results in Figure 16 illustrate that there is similar engine out CO_2 with all combustion and fuel strategies (except for low NO_x and noise CDC, which has ~20 g/mile higher emissions at all conditions) at all conditions (A–D). Interestingly, when E30+15% EGR is used in the downsize + downspeed approach

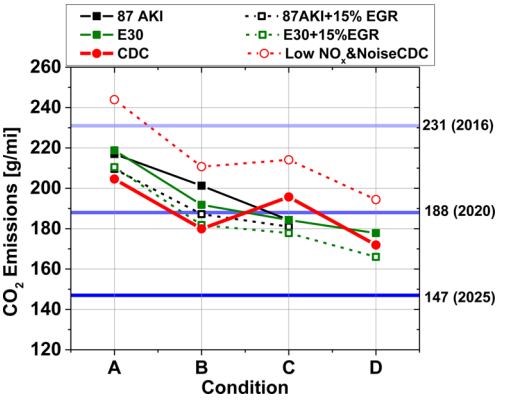

Figure 16. Estimated engine out CO_2 emissions MPG of each fuel and combustion strategy in a midsize sedan at a 65 MPH steady cruise condition.

dx.doi.org/10.1021/ef401574p | *Energy Fuels* XXXX, XXX, XXX–XXX

(condition D), there is up to a 23.5% reduction in CO_2 compared with 0% EGR 87AKI at condition A (similar to chassis dyno data of the production vehicle in Figures 14 and 15). It is noteworthy that the relative reserve power/torque of 87AKI in the 2.0 L engine at condition A is similar to that of the 1.2 L engine with E30+15% EGR at condition D. However, at these similar reserve torque conditions, the fuel economy of E30+15% EGR at condition D vs 87AKI at condition A was increased by 13.7% or 26.4% on an absolute and gasoline equivalent basis, respectively (Figures 14 and 15). These improvements are impressive relative to conventional SI and the production vehicle.

Since the SI and CDC engine power/torque densities become similar (especially in the range of 1600 r/min to 2500 r/min), a one-to-one comparison of conditions A, B, C, and D is possible. The unadjusted MPG of CDC vs E30+15% EGR is 33% higher at condition D and 40.6% higher at condition A. Assuming no significant differences in performance occur because of turbo lag emissions control strategies and EGR differences while using similar shift points and gearing, the theoretical drivability (transmission, shift points, reserve power, etc.) of these powertrain strategies would be similar. However, the EURO IV calibrated CDC engine is not US Tier 2 compliant in NO_x and soot emissions. Typically, reductions of these emissions hinder CDC fuel economy (as noted by the dashed low NO_x CDC data in Figures 15 and 16). Therefore, the present comparison likely biases the unadjusted MPG of CDC results to be somewhat higher in Figure 14. Nevertheless, the CDC engine shows higher MPG but with near identical engine-out CO_2 emissions (Figure 16).

DISCUSSION

The present study demonstrates that midlevel alcohol−gasoline blends such as IB24 and E30 have the potential to enable improvements in future engine designs. The results suggest that the use of midlevel alcohol blends, such as E30, open the door to extreme engine downsizing, with the potential for $\lambda = 1$ operation. If further pursued, extreme downsizing might require significant changes to the engine beyond the parameters investigated in the present study. For example, air-handling system(s) for downsized systems demand higher per unit displacement mass flow rates, requiring base engine and air-handling optimization. Likewise, heat transfer effects may be of greater importance in downsized platforms, as surface-to-volume relations scale as the square and cubic of bore and radius, respectively. The present study ignores these dimensional effects that could be present in application; however, the present findings demonstrate the general trends that could be expected with thorough and proper engineering of the base engine and supporting systems.

Although full engine testing and drive cycle analysis is not within the scope of the present study, the results demonstrate that midlevel ethanol−gasoline blends offer a substantial increase in fuel octane. The companion paper (part 2) addresses the fuel- and combustion-specific effects in greater detail and demonstrates that E30 has faster burning rates, lower adiabatic flame temperature, and improved knock tolerance.

This demonstrates that the engine's stoichiometric torque capability at high compression ratio could be doubled compared with that of 87AKI gasoline at the tested E30 blending ratio. The focus here is on engine efficiency, so a compression ratio of approximately 2 points higher than stock was used (11.85:1 vs 9.2:1). This biases the results toward higher octane fuels. However, if high engine efficiency is required to meet imposed CAFE standards in conjunction with the RFS II standards, then higher efficiency engines will be required. The results suggest how improvements to engine efficiency with simultaneous RFS II adoption could possibly use an integral approach with high-octane biofuels. While CAFE and EPA greenhouse gas legislation is intended to be aligned, both rely on a certification fuel, which is currently up for debate.[28] Sluder et al.[41] have recently illustrated that the relations between fuel ethanol content and the determination and weighting of vehicle fuel economy are important and that further thought may be required on the determination of certification fuels and adjusted mileage. Regardless of the fuel and final regulatory framework, the results here present a unique and infrequent opportunity to dramatically alter internal combustion engine operation by improving fuel properties.

Of particular note is that the present study uses steady-state engine testing with simulated air handling, a custom research piston design, a research valvetrain, and a friction correlation to estimate brake performance. Therefore, the physical MPG estimates are to be used as a guide and not as absolute in their magnitude. Additionally, production-level engineering and development are required beyond parameters investigated in the present analysis. For example, in downsized engine configurations, vehicle launch and turbo matching considerations are important. The transmission gearing and powertrain systems optimization are critical for both calibration and performance considerations at production levels. These factors are neglected in this analysis and can reduce the real MPG of downsized and or downspeed approaches. Finally, the MPG estimates in Figures 14−16 neglect "hotel" loads (i.e., cabin climate control systems, added electrical loads, etc.) that are encountered in actual vehicle operation, which directly affect fuel consumption. No attempt was made to estimate or compensate for these loads in the present analysis. Regardless of the assumptions, the present results illustrate that fuel properties are a promising and enabling technology for increasing engine efficiency for more energy-efficient vehicles.

CONCLUSIONS

The findings of this study are applicable to SI engine fuel economy and performance. Specifically, two midlevel alcohol blends, E30 and IB24, were compared with regular pump gasoline (87AKI) with 0% ethanol. The fuels were compared with 0 and 15% EGR at five speeds, from 2 bar IMEPg to a full-load condition, where either a combustion phasing or an EGT limit was met. The results demonstrate that E30 offers the highest stoichiometric torque capability at high compression ratio vs any other tested fuel, and with E30+15% EGR offering similar or higher power/torque density than a EURO IV CDC engine.

Engine efficiency was determined on a correlated brake and was measured on a net and gross basis. Regardless of the fuel type, 15% EGR increased BTE and NTE through reductions in throttling losses (PMEP) and increased GTE. GTE increased with 15% EGR for each fuel type. However, the specific operating limits and GTE benefits were observed to be fuel dependent, with 87AKI and IB24 receiving a higher relative improvement in GTE with 15% EGR. This is primarily because of 87AKI and IB24 receiving higher antiknock improvements with 15% EGR than E30. The increased knock suppression with 15% EGR in 87AKI gasoline enabled a similar stoichiometric torque capability at high compression ratio to IB24 without EGR but with a 1−2 absolute % increase in BTE. However, the overall GTE benefits

dx.doi.org/10.1021/ef401574p | Energy Fuels XXXX, XXX, XXX−XXX

of E30 were seen to be the highest in addition to expanding the maximum load at a given speed.

The combined findings demonstrate that midlevel ethanol blends—such as E30—open the potential for engine compression ratios and expanded downsize + downspeed powertrain approaches, providing clear pathways to improved vehicle fuel economy using existing engine technologies. The unique properties of midlevel alcohol−gasoline blends were shown to be the enabling technology toward higher engine efficiency, leading to feasible near-term increases in vehicle efficiency and reductions in CO_2. The present study focused only on the engine efficiencies, downsize, and downspeed possibilities with two intermediate alcohol−gasoline fuels. The study has not focused on the fact that IB24 and E30 are not currently market-available fuels or that to design mass production engines for them requires their market presence to be significantly increased. Regardless, the present findings demonstrate that, if adopted, intermediate alcohol−gasoline fuels, in particular E30, show promise as a means to increase vehicle efficiency in optimized SI engines.

AUTHOR INFORMATION

Corresponding Author

*E-mail: splitterda@ornl.gov.

Notes

Disclosure: This manuscript has been authored by the Oak Ridge National Laboratory, managed by UT-Battelle LLC under Contract No. DE-AC05-00OR22725 with the U.S. Department of Energy. The U.S. Government retains and the publisher, by accepting the article for publication, acknowledges that the U.S. Government retains a nonexclusive, paid-up, irrevocable, worldwide license to publish or reproduce the published form of this manuscript, or allow others to do so, for U.S. Government purposes.

The authors declare no competing financial interest.

†E-mail: szybistjp@ornl.gov.

ACKNOWLEDGMENTS

The authors gratefully acknowledge the support of the U.S. Department of Energy, particularly Kevin Stork and Steve Przesmitzki of the Office of Vehicle Technologies. Additionally, the authors would like to acknowledge John Thomas for his assistance with road load calculations and Vicki Kalaskar for assistance with the engine test laboratory.

ABBREVIATIONS

EPA, U.S. Environmental Protection Agency; RFS II, Renewable Fuels Standard II; CAFE, corporate average fuel economy; SI, spark ignition; LD, light duty; NO_x, oxides of nitrogen; CO, carbon monoxide; HC, hydrocarbon; HoV, enthalpy of vaporization; MPG, miles per gallon; EGR, exhaust gas recirculation; λ, lambda; γ, ratio of specific heats; HVA, hydraulic valve actuation; CA, crank angle; FSN, filter smoke number; AFR, air fuel ratio; $ATDC_f$, after top dead center firing; ATDC, after top dead center; $IMEP_g$, indicating mean effective pressure gross; RON, research octane number; MON, motor octane number; LHV, lower heating value; GTE, gross thermal efficiency; HRR, heat release rate; CA50, crank angle at 50% mass fraction burned; AKI, antiknock index; E30, 30% ethanol and gasoline by volume; E0, 0% ethanol by volume; IB24, 24% isobutanol and gasoline by volume; CO_2, carbon dioxide; CDC, conventional diesel combustion; FMEP, friction mean effective pressure; PMEP, pumping mean effective pressure; NTE, net thermal efficiency; BMEP, brake mean effective pressure; BTE, brake thermal efficiency; LSPI, low speed preignition; DI, direct injection; MBT, maximum brake torque; BOB, blendstock for oxygenate blends; GT Power, Gamma Technologies Power

REFERENCES

(1) One Hundred Tenth Congress of the United States of America, Energy Independence and Security Act of 2007. 2007; H.R. 6.

(2) U.S. Environmental Protection Agency, "40 CFR Part 80 Regulation of Fuels and Fuel Additives: 2011 Renewable Fuel Standards; Final Rule", http://www.gpo.gov/fdsys/pkg/FR-2010-12-09/pdf/2010-30296.pdf, accessed May 2, 2013.

(3) Energy information agency transportation sector energy consumption report, http://www.eia.gov/totalenergy/data/monthly/#consumption, accessed May 2, 2013.

(4) National Highway Traffic Safety Administration and Environmental Protection Agency, "2017 and Later Model Year Light-Duty Vehicle Greenhouse Gas Emissions and Corporate Average Fuel Economy Standards; Final Rule", http://www.nhtsa.gov/fuel-economy, accessed May 2, 2013.

(5) U.S. Environmental Protection Agency, "Light-Duty Automotive Technology, Carbon Dioxide Emissions, and Fuel Economy Trends: 1975 Through 2012", http://www.epa.gov/fueleconomy/fetrends/1975-2012/420r13001.pdf, accessed May 2, 2013.

(6) Fraser, N.; Blaxill, H.; Lumsden, G.; Bassett, M. Challenges for Increased Efficiency through Gasoline Engine Downsizing. *SAE Int. J. Engines* **2009**, *2* (1), 991−1008, DOI: 10.4271/2009-01-1053.

(7) Stein, R.; Polovina, D.; Roth, K.; Foster, M. Effect of Heat of Vaporization, Chemical Octane, and Sensitivity on Knock Limit for Ethanol−Gasoline Blends. *SAE Int. J. Fuels Lubr.* **2012**, *5* (2), 823−843, DOI: 10.4271/2012-01-1277.

(8) Stein, R.; House, C.; Leone, T. Optimal Use of E85 in a Turbocharged Direct Injection Engine. *SAE Int. J. Fuels Lubr.* **2009**, *2* (1), 670−682, DOI: 10.4271/2009-01-1490.

(9) Szybist, J.; Foster, M.; Moore, W.; Confer, K. Investigation of Knock Limited Compression Ratio of Ethanol Gasoline Blends. *SAE Technical Paper 2010-01-0619*; 2010; DOI: 10.4271/2010-01-0619.

(10) Szybist, J. P.; Chakravathy, K.; Daw, C. S. Analysis of the Impact of Selected Fuel Thermochemical Properties on Internal Combustion Engine Efficiency. *Energy Fuels* **2012**, *26* (5), 2798−2810, DOI: 10.1021/ef2019879.

(11) Stein, R.; Anderson, J.; Wallington, T. An Overview of the Effects of Ethanol-Gasoline Blends on SI Engine Performance, Fuel Efficiency, and Emissions. *SAE Int. J. Engines* **2013**, DOI: 10.4271/2013-01-1635.

(12) Jung, H.; Shelby, M.; Newman, C.; Stein, R. Effect of Ethanol on Part Load Thermal Efficiency and CO_2 Emissions of SI Engines. *SAE Int. J. Engines* **2013**, DOI: 10.4271/2013-01-1634.

(13) Jung, H.; Leone, T.; Shelby, M.; Anderson, J. Fuel Economy and CO_2 Emissions of Ethanol-Gasoline Blends in a Turbocharged DI Engine. *SAE Int. J. Engines* **2013**, DOI: 10.4271/2013-01-1321.

(14) Szybist, J.; West, B. The Impact of Low Octane Hydrocarbon Blending Streams on the Knock Limit of "E85". *SAE Int. J. Fuels Lubr.* **2013**, *6* (1), 44−54, DOI: 10.4271/2013-01-0888.

(15) Anderson, J. E.; Kramer, U.; Mueller, S. A.; Wallington, T. J. Octane Numbers of Ethanol− and Methanol−Gasoline Blends Estimated from Molar Concentrations. *Energy Fuels* **2010**, *24* (12), 6576−6585, DOI: 4134154/ef101125c.

(16) Anderson, J.; Leone, T.; Shelby, M.; Wallington, T., et al. Octane Numbers of Ethanol-Gasoline Blends: Measurements and Novel Estimation Method from Molar Composition. SAE Technical Paper 2012-01-1274; 2012; DOI: 10.4271/2012-01-1274.

(17) Foong, T. M.; Morganti, K. J.; Brear, M. J.; da Silva, G.; Yang, Y.; Dryer, F. L. The octane numbers of ethanol blended with gasoline and its surrogates. *Fuel* **2014**, *115*, 727−739.

(18) High Octane Fuel Symposium, International Society of Automotive Engineers, January 2013, Washington, DC, http://www.sae.org/events/hofs/.

(19) Alger, T.; Mangold, B.; Roberts, C.; Gingrich, J. The Interaction of Fuel Anti-Knock Index and Cooled EGR on Engine Performance and Efficiency. *SAE Int. J. Engines* **2012**, *5* (3), 1229−1241, DOI: doi:10.4271/2012-01-1149.
(20) Wheeler, J.; Polovina, D.; Ramanathan, S.; Roth, K. Increasing EGR Tolerance using High Tumble in a Modern GTDI Engine for Improved Low-Speed Performance. *SAE Technical Paper 2013-01−1123*; 2013; DOI: 10.4271/2013-01-1123.
(21) Alger, T.; Gingrich, J.; Mangold, B.; Roberts, C. A Continuous Discharge Ignition System for EGR Limit Extension in SI Engines. *SAE Int. J. Engines* **2011**, *4* (1), 677−692, DOI: 10.4271/2011-01-0661.
(22) Splitter, D. A.; Szybist, J. P. Intermediate Alcohol-Gasoline Blends. Fuels for Enabling Increased Engine Efficiency and Powertrain Possibilities. *SAE Technical Paper 2014-10-1231,* **2014**, DOI: 10.4271/2014-01-1231.
(23) Szybist, J.; Nafziger, E.; Weall, A. Load Expansion of Stoichiometric HCCI Using Spark Assist and Hydraulic Valve Actuation. *SAE Int. J. Engines* **2010**, *3* (2), 244−258, DOI: 10.4271/2010-01-2172.
(24) Weall, A.; Szybist, J.; Edwards, K.; Foster, M.; et al. HCCI Load Expansion Opportunities Using a Fully Variable HVA Research Engine to Guide Development of a Production Intent Cam-Based VVA Engine: The Low Load Limit. *SAE Int. J. Engines* **2012**, *5* (3), 1149−1162, DOI: 10.4271/2012-01-1134.
(25) Heywood, J. B. *Internal Combustion Engine Fundamentals*; McGraw-Hill: New York, 1988.
(26) Federal Register, Vol. 75 (213), Thursday, November 4, 2010, Notices.
(27) Federal Register, Vol. *76* (17), Wednesday, January 26, 2011, Notices.
(28) U.S. Environmental Protection Agency. Proposed ruling, "Control of Air Pollution from Motor Vehicles: Tier 3 Motor Vehicle Emission and Fuel Standards", http://www.epa.gov/otaq/tier3.htm, accessed May 2, 2013.
(29) National Renewable Energy Laboratory Report, "Utilization of Renewable Oxygenates as Gasoline Blending Components", http://www.nrel.gov/docs/fy11osti/50791.pdf, accessed May 2, 2013.
(30) American Petroleum Institute. *Alcohols and Ethers, A Technical Assessment for Their Application as Fuels and Fuel Components*, 3rd ed.; API: June 2001; p 4261.
(31) Wilhoit, R. C.; Zwolinski, B. J. Physical and Thermodynamic Properties of Aliphatic Alcohols. *J. Phys. Chem. Ref. Data*, **1973**, Vol. *2*, Supplement No. 1.
(32) Splitter, D. A.; Szybist, J. P. An Experimental Investigation of Spark Ignited Combustion With High Octane Bio-Fuels and EGR, Part 2 of 2 Fuel and EGR Effects on Konck Limited Load and Speed. *Energy Fuels* **2013**, DOI: 10.1021/ef401575e.
(33) Gamma Technologies. *GTPower Suite 4 Users Manual*; 2012.
(34) Caton, J. A Comparison of Lean Operation and Exhaust Gas Recirculation: Thermodynamic Reasons for the Increases of Efficiency. *SAE Technical Paper 2013-01−0266*; 2013; DOI: 10.4271/2013-01-0266.
(35) EPA Test Car List Data Files, http://www.epa.gov/otaq/tcldata.htm, accessed May 2, 2013.
(36) Curran, S.; Hanson, R.; Wagner, R.; Reitz, R. Efficiency and Emissions Mapping of RCCI in a Light-Duty Diesel Engine. *SAE Technical Paper 2013-01−0289*; 2013; DOI: 10.4271/2013-01-0289.
(37) Amann, M.; Alger, T.; Mehta, D. The Effect of EGR on Low-Speed Pre-Ignition in Boosted SI Engines. *SAE Int. J. Engines* **2011**, *4* (1), 235−245, DOI: 10.4271/2011-01-0339.
(38) Thomas, J. F.; Hwang, H.-L.; West, B.; Huff, S. Predicting Light-Duty Vehicle Fuel Economy as a Function of Highway Speed. *SAE Int. J. Passeng. Cars—Mech. Syst.* **2013**, DOI: 10.4271/2013-01-1113.
(39) Thomas, J. Oak Ridge National Laboratory, private communication, September 2013.
(40) U.S. Environmental Protection Agency. Final Technical Support Document: "Fuel Economy Labeling of Motor Vehicle Revisions to Improve Calculations of Fuel Economy Estimates, EPA420-R-06-017, December 2006.
(41) Sluder, S.; West, B.; Butler, A. D.; Arvon, M. L.; Ruona, W. Determination of the R Factor for Fuel Economy Calculations Using Ethanol-Blended Fuels Over Two Test Cycles. *SAE Technical Paper 2014-10-1572,* **2014**, DOI: 10.4271/2014-01-1572.